The structure and properties of poly(hexamethylene terephthalate): 1. The preparation, morphology and unit cells of three allomorphs

I. H. Hall and B. A. Ibrahim*
Department of Pure and Applied Physics, UMIST, PO Box 88, Manchester M60 1QD, UK
(*Received* 20 *July* 1981)

Poly(hexamethylene terephthalate) is shown to crystallize in one of three possible allomorphs. Two of these have been found in material crystallized from the melt, but neither has been produced in the pure state. One (the α-phase) is favoured when crystallization occurs under stress and is found in fibrillar materials, the other (the β-phase) is favoured by high-temperature, relaxed, annealing, and is found in spherulitic material. Where there is a high proportion of α-phase present, the β-phase appears to grow epitaxially on it. The third phase (the γ-phase) has only been found in material crystallized from solution at room temperature, and is converted to the other phases by annealing or orientation. All three phases have the same crystallographic repeat along the chain axis, which corresponds to a nearly fully extended conformation. They must therefore differ principally in the way chains pack together. The α-phase unit cell is monoclinic, the other two are triclinic. All unit cell parameters are given.

Keywords Structure; poly(hexamethylene terephthalate); preparation; morphology; unit cells; allomorphs; crystallization

INTRODUCTION

Of recent years, the structures and properties of the family of fibrous polymers having the chemical formula

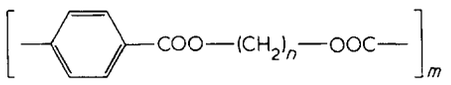

have been receiving systematic attention. These are poly(*n*-glycol terephthalate) (*n*-GT), where *n* is the number of methylene units. So far, detailed information is available on the polymers from $n=2$ to $n=5$, and from these studies two features have emerged. The methylene sequence is not always all-*trans*, and in some of these cases where it is not it may undergo a reversible, stress-induced phase transition into the all-*trans* conformation. Thus the three methylene bonds in 4-GT have the sequence $\bar{G}TG$[1-3]. Under stress this transforms to an all-*trans* sequence[1,2,4,5], reverting to the original conformation when stress is released. A theory of cooperative first-order phase transitions[6] and certain features of the stress–strain curve and of recovery from strain have been related to this transition[4,7].

With 5-GT the situation is more complicated. If a fibre is annealed in the stress-free state, the methylene sequence is not all-*trans*, though the conformation angles seem to differ significantly from the *gauche* value[8,9]. Under stress, transformation occurs to the all-*trans* conformation, and if the specimen is annealed whilst under stress, a proportion of the chains will remain in this state when stress is released. It is only after annealing in the stress-free state that all the crystallites of an unstressed fibre have chains in the same conformation.

The two methylene bonds of 3-GT are both *gauche*[10,11] but an all-*trans* conformation has not been produced although the mechanical and thermal treatments which have caused transformation in 4- and 5-GT have been tried. 2-GT is all-*trans*[12], and there are no reports of any other conformation.

Goodman[13] has reported the crystallographic repeat length of 6-GT and two unit-cell determinations have been published[14,15]. All these indicate that the methylene sequence must be all-*trans*. Bateman *et al.*[14] refer to several weak reflections in the X-ray diffraction pattern which cannot be indexed on their unit cell and Schenk[16] points out that the unit-cell density is less than that of the bulk specimen. Joly *et al.*[15] make no reference to these reflections and their unit-cell density is considerably higher than the bulk value. Schenk has also shown that the diffraction patterns of samples crystallized from solution are different from those crystallized from the melt, indicating the existence of two polymorphs of the material.

We have been studying this material, and, following from the experience of other members in the series, have been looking for polymorphic forms. In a preliminary report[17] we have shown that material will crystallize from the melt into two distinct phases. Normally both are present and their properties depend on drawing speed. Both have the same crystallographic repeat. The present paper reports a more detailed study of the conditions preferred for the crystallization of a particular phase. The unit cells are also given and the morphology of the different phases is discussed.

* Present address: 8d/56 Raghiba Khatoon, Baghdad, Iraq

0032-3861/82/060805-12$03.00

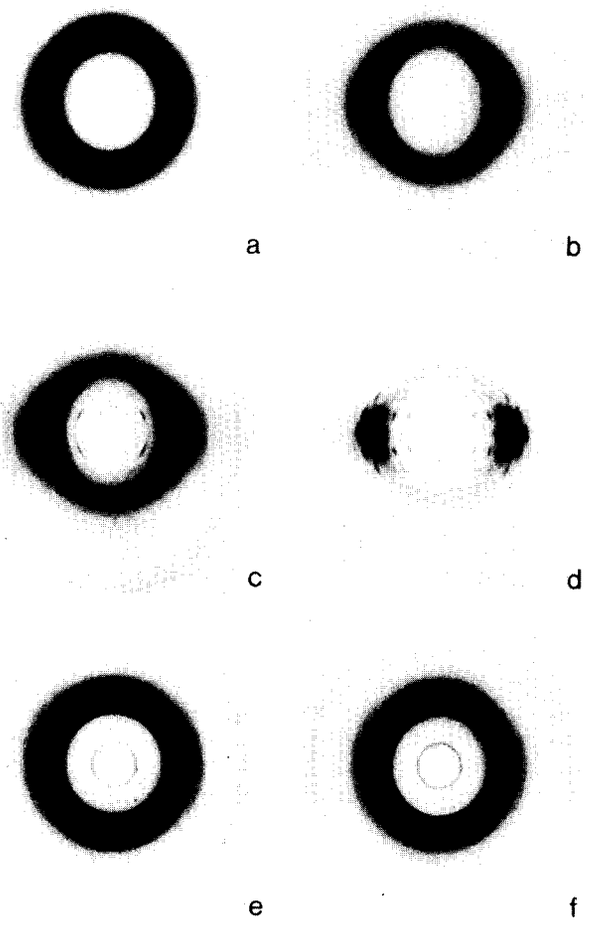

Figure 1 Diffraction patterns of as-spun fibres: (a) Gravitationally spun; (b) take-up speed of 50 m min^{-1}; (c) take-up speed of 150 m min^{-1}; (d) take-up speed of 400 m min^{-1}; (e) gravitationally spun – low molecular weight material; (f) gravitationally spun – collected 40 cm below spinnaret

PRODUCTION OF VARIOUS POLYMORPHS

In a previous publication[17], the existence of two phases in melt-spun material was reported. One phase, called the α-phase, was obtained by hand-drawing. This phase persisted when the material was subsequently annealed at constant length. Fibres which are drawn over a hot plate at 80°C and subsequently annealed at 145°C were in a different phase, called the β-phase. More generally, fibres comprised a mixture of both phases. High speed drawing at low temperatures favoured the α-phase, slow drawing at higher temperatures and subsequent annealing favoured the β-phase. These investigations were hampered because only material of relatively low molecular weight (intrinsic viscosity 0.528 dl/g when dissolved in chloroform) was available which was difficult to spin and draw. For the present investigation, higher molecular weight material had become available (intrinsic viscosity 0.93 dl/g when dissolved in chloroform) and this enabled a more thorough study of the effects of spinning and drawing conditions to be made.

Effect of spinning conditions

The high molecular weight polymer was dried for 48 h in an evacuated oven at 85°C. It was then transferred to the cylinder of a spinning machine and candled at 132°C, after which the temperature was raised to 168°C and held at that value for about 10 min before extrusion through an orifice of 0.5 mm diameter was commenced. One extruded monofilament was allowed to fall freely to the ground, a distance of approximately 9 m (called gravitationally spun) and others were collected at take-up speeds of 50, 150, 300 and 400 m min^{-1}. The X-ray diffraction patterns of six of these fibres are shown in *Figure 1*. These were taken on a cylindrical film coaxial with the fibre using Cu Kα radiation in an evacuated camera. From this figure it will be seen that the gravitationally spun fibre is unoriented and that orientation increases with take-up speed until the fibre collected at 400 m min^{-1} is quite highly oriented. This is expected; what is unexpected is the change in relative intensities of some of the reflections. For example, in *Figure 1a* relating to the gravitationally spun fibre the innermost diffraction ring is more intense than the next. These two rings correspond to the innermost reflections on the first layer line. It is seen that as take-up speed increases, the first of these reflections becomes weaker and the second more intense. The intensity distribution at 400 m min^{-1} is similar to that for the α-phase (see ref 17); that for the gravitationally spun fibre corresponds to the β-phase. The most likely explanation of these results is that the phase which crystallizes depends on spin-line tension. At constant extrusion rate the spin-line tension will increase with take-up speed and a high tension will favour production of the α-phase.

To confirm this, a lower molecular weight material (intrinsic viscosity 0.344 dl/g when dissolved in chloroform) was spun and collected under gravity. The second ring was absent from the diffraction pattern (*Figure 1e*) which would be expected if the tension was still lower than that as for *Figure 1a*. In a further experiment the higher molecular weight material was spun and collected under gravity but at a height of only 40 cm below the spinnaret (compared with 9 m for that allowed to fall to the floor). This would also reduce the tension and the second ring was again missing from the diffraction pattern (*Figure 1f*) confirming that this reflection is absent from the β-phase, and that this will only crystallize in the pure form at very low tensions. The material is, however, unoriented so the slight orientation visible in the diffraction pattern of the lower molecular weight material (*Figure 1e*) remains unexplained.

Effect of drawing and annealing

The diffraction pattern of a drawn material was too diffuse to conclude anything about the structure; thus the effects of drawing and annealing had to be studied together.

Gravitationally spun fibre, and that collected at 50 and 400 m min^{-1} was drawn at room temperature on an 'Instron' tensile testing machine at various cross-head speeds from 0.5 to 100 cm min^{-1} and to draw ratios (measured from the jaw separation) between 2 and 8. Drawing at 85°C was also performed on an 'Instron' over a similar range of cross-head speeds and draw ratios, but on gravitationally spun fibre only. This fibre was also drawn over a hot plate at 50°C to draw ratios of 4 and 8 as measured by the speeds of the delivery and take-up bobbins.

Samples of each of the fibres produced in this way, and of the undrawn fibre, were annealed at temperatures between 80°C and the melting point (approximately

160°C) and their X-ray diffraction pattern recorded. Annealing was performed for 2 h in air followed by quenching in air at room temperature, the fibre being held at constant length throughout.

From these experiments it was clear that the materials could be divided into two groups, and that there were three ranges of annealing temperature (80° to 100°C, 110° to 135°C, and 140°C to the melting point) in each of which characteristic behaviour was exhibited. The first group of materials comprised cold- and hot-drawn fibres with loe draw ratio and as-spun fibre with low take-up velocity, the second comprised hot- and cold-drawn fibre with high draw ratios and as-spun fibre with high take-up speed. In the subsequent discussion a gravitationally spun fibre, drawn on an 'Instron' to a draw ratio of 4 will be taken as representative of the first group, and an as-spun fibre collected with a take-up speed of 400 m min^{-1} as representative of the second.

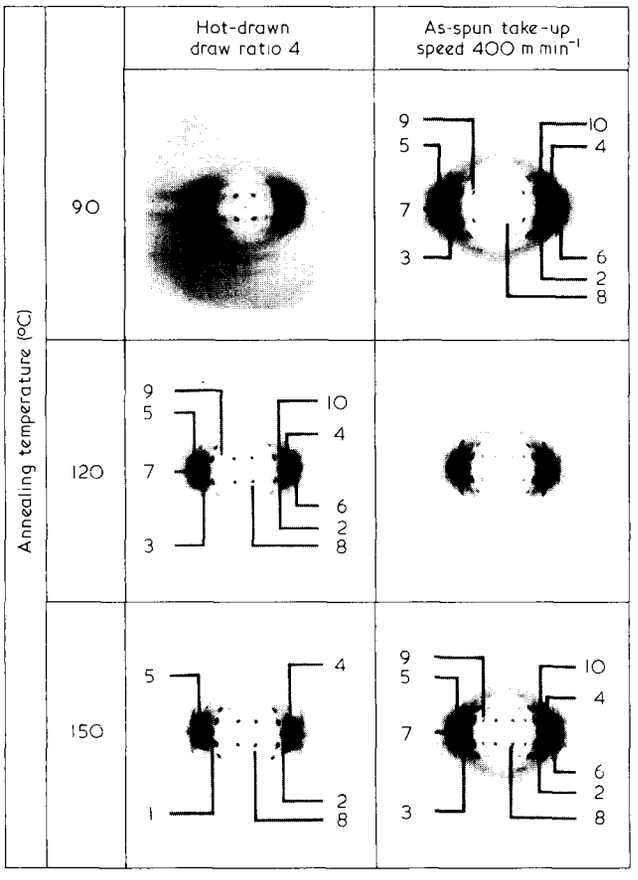

Figure 2 Effect of drawing and annealing on diffraction pattern (The numbered reflections are given in *Table 1*)

In *Figure 2* the diffraction patterns of each of these are shown after annealing at 90 C, 120 C and 150 C. Within these broad classifications, individual fibres showed small variations of behaviour which will be discussed later.

Annealing at 90 C simply had the effect of increasing the intensity and resolution of the diffraction pattern. This trend continued at 120 C but certain reflections had changed in intensity in a different way from others. The most noticeable of these have been numbered in the figure. At 150°C these changes in relative intensity had stabilized and further increase in temperature produced no further change.

The changes in the relative intensities (estimated by eye) of the numbered reflections are given in *Table 1*. For a hot-drawn material the intensities of reflections 1, 2, 5 and 8 increase, whereas those of the others decrease, some of them eventually disappearing. For the other material the intensity of all reflections has increased, the greatest increases occurring in those which also increased in the first.

Thus for materials in the first group, as the annealing temperature is increased some reflections grow in intensity, others decay or disappear. This suggests that a crystal structure present before annealing is being melted and a different structure, possibly also present in the unannealed material is crystallizing. However for materials in the second group some reflections again grow in intensity faster than others, but none decay indicating development of the crystallinity of one phase with increasing temperature, but without melting of the other.

Comparisons of coordinates of reflections show that the phase which develops with high temperature annealing has the same structure in both materials and is that which we have previously called the β-phase. That which is melted in materials of the first group but remains in the others also has the same structure in both and is that which we called the α-phase. Thus it would appear that in the first group both α- and β-phases are initially present but annealing melts the α-phase crystallites which recrystallize as β-phase. In the other materials, only α-phase crystallites exist before annealing and these remain upon annealing. The β-0hase must crystallize from initially amorphous material.

Within this broad pattern of experimental behaviour there are small individual variations. Thus in the highest temperature annealing range, the particular temperature at which a given pattern is obtained for fibres in the same group depends upon their history and, for the fibre collected at a take-up speed of 50 m min^{-1} this temperature is higher than for the gravitationally spun, but is lower than for the cold drawn.

Table 1 Relative intensities of reflections

	Hot-drawn		Spun with take-up speed of 400 m min^{-1}	
Reflection No.	Annealed 90°C	Annealed 150°C	Annealed 90°C	Annealed 150°C
1	Diffuse	Medium	–	–
2	Medium	Intense	Very faint	Medium
3	Medium	–	Medium	Medium
4	Very intense	Intense	Very intense	Very intense
5	Very intense	Very intense	Medium	Very intense
6	Medium	Faint	Medium	Medium
7	Medium	Faint	Medium	Medium
8	Medium	Very intense	Faint	Intense
9	Medium	Very faint	Medium	Medium
10	Medium	–	Medium	Medium

Table 2 Effects of drawing and annealing on proportions of α- and β-phases

Sample type	As-prepared	Annealed 80°–100°C	Annealed 110°–135°C	Annealed 140°–150°C	Melted ~162°C
A	$\alpha = \beta$	$\alpha \leqslant \beta$	$\alpha \leqslant \beta$	β-form	β-form
B	$\alpha > \beta$	$\alpha = \beta$	$\alpha \leqslant \beta$	β-form	β-form
C	α-form	$\alpha \gg \beta$	$\alpha \geqslant \beta$	$\alpha \leqslant \beta$	β-form
D	$\alpha = \beta$	$\alpha = \beta$	$\alpha < \beta$	$\alpha \ll \beta$	β-form
E	pattern diffuse	$\alpha > \beta$	$\alpha \geqslant \beta$	$\alpha = \beta$	β-form
F	pattern diffuse	$\alpha \gg \beta$	$\alpha > \beta$	$\alpha \geqslant \beta$	β-form

Key to sample types
A – Gravitationally spun
B – As-spun, take-up speed 50 m min^{-1}
C – As-spun, take-up speed 400 m min^{-1}
D – Gravitationally spun, then cold-drawn at 0.5–5 cm min^{-1} (DR ~4) or hot-drawn at 1–100 cm min^{-1} (DR ~4)
E – Gravitationally spun, then cold-drawn at 50–100 cm min^{-1} (DR ~4.5) or hot-drawn at 1–100 cm min^{-1} (DR ~8). Also spun with take-up speed 50 m min^{-1} then cold-drawn at 5–100 cm min^{-1} (DR ~3)
F – Gravitationally spun, then cold-drawn at 1–100 cm min^{-1} (DR ~7.5) or hot-drawn by machine at 240 cm min^{-1} (DR ~8). Also spun with take-up speed of 50 m min^{-1}, cold-drawn at 5–100 cm min^{-1} (DR ~5) and spun with take-up speed of 400 m min^{-1}, cold-drawn at 5–100 cm min^{-1} (DR ~2)

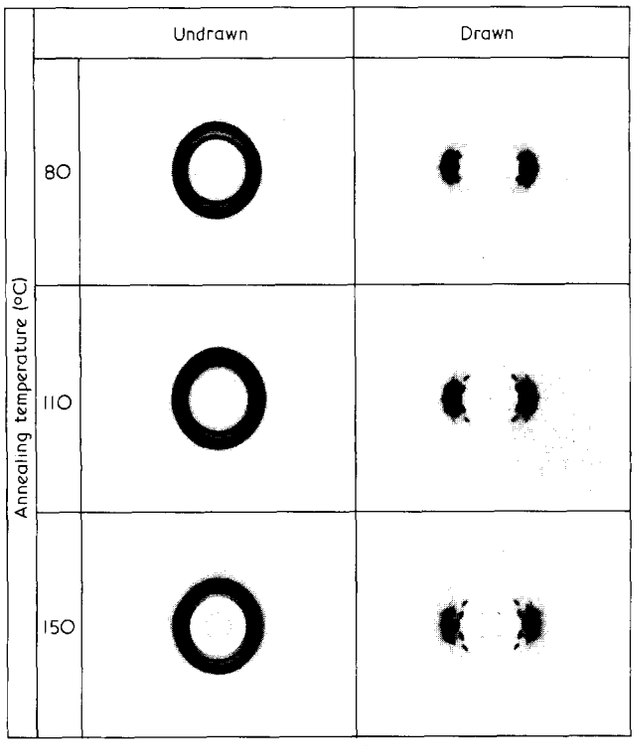

Figure 3 Diffraction patterns of cast film

Tension during annealing was also found to be important. A fibre annealed at 140°C whilst free to retract showed a greater proportion of β-phase than one annealed at constant length. On the other hand, if it was annealed under constant tension a greater proportion of the α-phase would remain.

In a previous paper[17] we suggested that a high speed of drawing caused a high proportion of α-phase. However, increasing speed of drawing will also tend to increase both the draw ratio and the tension under which drawing occurs. With the higher molecular weight material available for the present study we have been able to reproduce similar draw ratios at different drawing speeds, and these tests have shown that it is a high draw ratio rather than a high drawing speed which causes preferential production of the α-phase. On the other hand comparison of the hot-drawn and as-spun diffraction patterns in *Figure 2* reveals that in the latter the crystallites tend to be less well orientated than in the former, even though the α-phase predominates.

Thus it would appear that the important parameter determining which phase crystallizes is the stress under which it nucleates. Under high stress conditions, well-formed α-phase crystallites will nucleate and will remain on annealing. Additional crystallization during annealing will be predominantly in the β-phase, though under a high stress further α-phase will develop. This is the behaviour of the second group of materials. If there is little stress present, any α-phase crystallites which nucleate will be imperfect and melt during subsequent annealing, recrystallizing into the β-phase. This is the behaviour demonstrated by the first group of materials.

The results of all experiments are summarized in *Table 2*, which sustains the above hypothesis.

Experiments with cast films

The high molecular weight polymer was dissolved in chloroform (2 g to 50 ml) which was allowed to evaporate in air at room temperature. Part of the resulting film was drawn by hand to a draw ratio of approximately 2.5. The X-ray diffraction patterns of both drawn and undrawn films were recorded before annealing, and after annealing to temperatures between 80°C and the melting point. In *Figure 3*, the patterns are shown of each film after annealing at 80°C, 110°C and 150°C. The crystalline structure of the drawn film which has been annealed at 80°C is in neither the α- nor β-phase. We propose to call this the γ-phase. The *d*-spacings in the undrawn material are the same as in the drawn, so this is presumably also in the γ-phase.

Further experiments, in which the solution was precipitated by adding methanol at room temperature, yielded the γ-phase. Alternatively, either annealing this phase at 100° to 150°C or evaporating the solution at 90°C yields only the β-phase.

Thus a third phase of this material exists which is obtained by crystallization from solution at room temperature. Annealing this phase at temperatures in the range 100°–150°C, or crystallization at 90°C will yield the β-phase.

MORPHOLOGY OF THE VARIOUS ALLOMORPHS

Small-angle X-ray scattering

To study the morphology of the various allomorphs

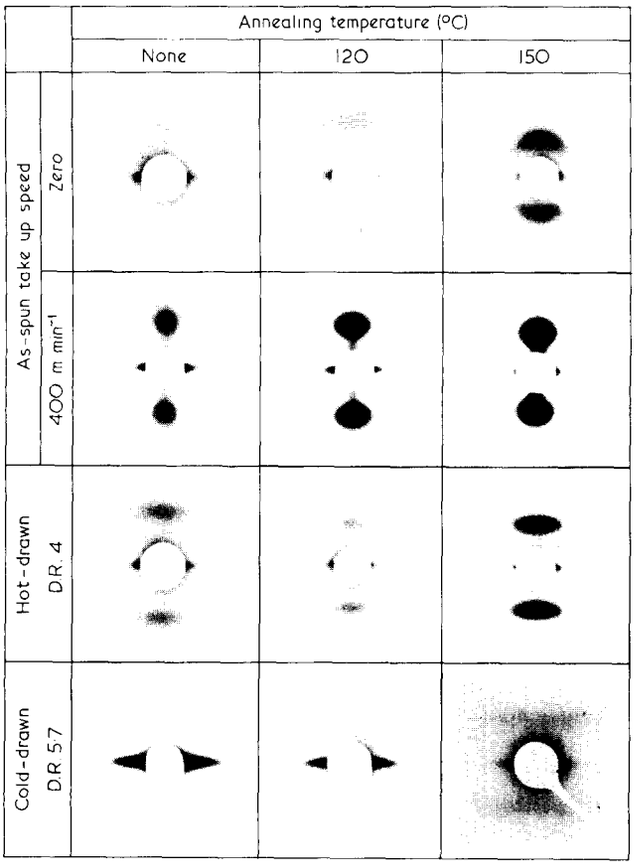

Figure 4 Small-angle diffraction patterns

four fibres were chosen whose proportions of α- and β-phases had been characterized in the experiments just described, and are given in *Table 2*. These fibres were:

(a) gravitationally spun,
(b) as-spun with a take-up speed of 400 m min^{-1},
(c) hot-drawn to a draw ration of 4, and
(d) cold-drawn at 100 cm min^{-1} to a draw ration of 5.7.

The specimens were annealed in air for 2 h at various temperatures whilst held at constant length and the small-angle X-ray diffraction patterns recorded. A selection of these is shown in *Figure 4*. The photographs were taken using a Rigaku–Denki goniometer with pin-hole collimation. The samples chosen were of such a thickness as to give a satisfactory exposure in 24 h unless otherwise stated.

It is seen that before annealing the four samples all show different patterns. For the gravitationally spun fibre it is a diffuse ring with slight maxima on the meridian indicating slight orientation (this required 45 h exposure); the other as-spun fibre consists of two discrete meridional points. The hot-drawn fibres showed horizontal reflections on the meridian, but no discrete reflections were apparent for the cold-drawn, even after 100 h exposure. Equatorial streaks are visible on all patterns, especially for the highly oriented materials. These are probably due to longitudinal voids.

On annealing in the range 110°–135°C the intensity of all patterns increases, and for the cold-drawn fibre a weak, four-point, pattern has appeared. Annealing between 140°C and the melting point will further increase the intensity of the patterns of the gravitationally spun and hot-drawn fibres, but increase those of the other two to a much lesser extent.

The previous experiments have shown that any α-phase present in the gravitationally spun and hot-drawn fibres will disappear on annealing and the amount of β-phase will increase. Both of these materials have a pronounced small angle reflection which grows in intensity with increasing annealing temperature. This indicates the development of a chain-folded lamellar structure and so it seems that the β-phase will occur when crystallization is chain-folded.

For the other two materials the amount of α-phase present remains constant on annealing, or increases slightly, but the amount of β-phase increases. Thus for the cold-drawn material it would appear that the α-phase comprises chain-extended crystals and that the developing β-phase causes the appearance of the four-point pattern. The separation of the points on this pattern indicates that the lamellae faces have normals at 38° to the chain axes. The normal to the *a*, *b* plane of the β-phase unit cell (to be given in the next section) is at 37.3° to the *c*-axes. This strongly suggests that the β-phase crystals grow epitaxially onto the α-phase. Since the α-phase does not melt, there are limitations to the extent to which this structure can develop and the intensity of the pattern does not increase at high annealing temperature. The meridional reflection observed with the spun fibre collected at high take-up speed is indicative of chain-folding, but it is different in character from the other meridional reflections and does not grow in intensity with annealing at high temperatures. Its shape after annealing at 150°C is indicative of a wide range of periodicities extending to high values, and is thus suggestive of fibrillar structure with irregular lamellar overgrowth.

The long period of each sample was estimated using Bragg's law and these are plotted against annealing temperature in *Figure 5*. From this it is seen that the long-spacing increases with annealing temperature for all fibres, though the rate of increase is different for the drawn fibres than for the gravitationally spun. In this respect, the as-spun fibre collected at high take-up speed behaves similarly to drawn fibres in the lower temperature range, and to the gravitationally spun in the upper part. The long

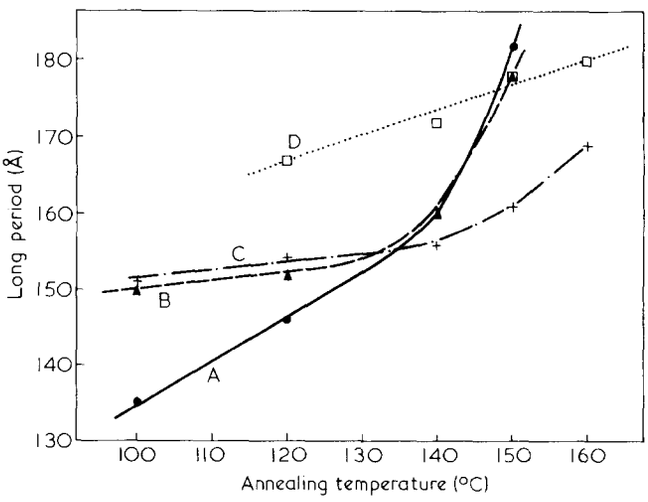

Figure 5 Effect of annealing temperature on long spacing. (A) Gravitationally spun; (B) spun with take-up speed of 400 m min^{-1} (C) hot-drawn; (D) cold-drawn

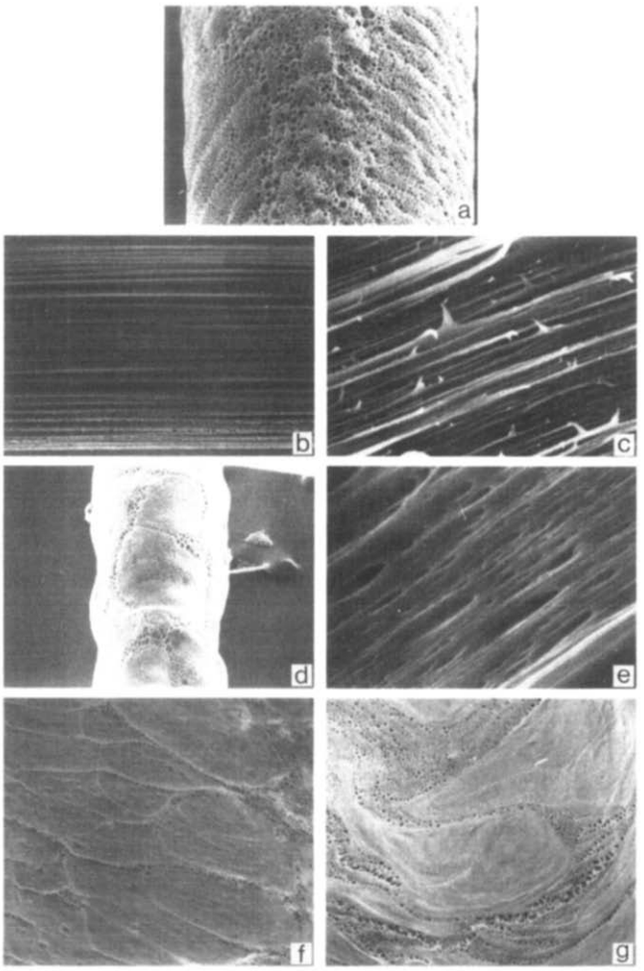

Figure 6 Scanning electron micrographs: (a) etched surface of gravitationally spun fibre; (b) etched surface of fibre cold-drawn to draw ratio of 5; (c) internal structure of fibre cold-drawn to draw ratio of 5; (d) etched surface of fibre hot-drawn to draw ratio of 4; (e) internal structure of fibre spun with take-up speed of 400 m min^{-1}; (f) etched surface of hot-drawn film; (g) etched surface of cold-drawn film

period of the cold-drawn material is greater than that of the hot-drawn at all annealing temperatures and at higher temperatures is similar to that of the other two materials.

Thus the magnitude of the long-spacing, and its change on annealing, do not seem to be associated with the properties of α- and β-phase present.

Scanning electron microscopy

Scanning electron micrographs were taken of the surface of gravitationally spun, hot- and cold-drawn fibre, both before and after etching in chloroform for 2 s. They were also taken of the surface of etched hot- and cold-drawn films. The interior structure of spun (with high take-up velocity) and cold-drawn fibres was made visible by peeling under liquid nitrogen. A selection of the photographs is shown in *Figure 6*.

The surface pictures of the cold-drawn fibres are indicative of a fibrillar structure, as are those of the interior of the cold-drawn and spun fibres. The fibrils are oriented along the fibre axis, and there are also indications of voids between the fibrils. The gravitationally spun material shows no surface structure but the hot-drawn fibres and films could be spherulitic. The cold-drawn films are also spherulitic though these are now severely deformed.

Thus the results are consistent with the conclusions from small angle scattering. Those materials which retain their α-phase crystallites on annealing are fibrillar suggesting that these crystallites may be chain extended, whereas those which are transformed to β-phase are spherulitic, making chain-folding likely on annealing.

Studies on single crystals

Brisse[18] has precipitated single crystals from solution and obtained transmission electron micrographs and diffraction patterns from them. Two distinct types of crystal were obtained, one was a platelet, the other fibrillar, and they produced different diffraction patterns.

UNIT-CELL DETERMINATION

Unit-cell determination was made difficult because it was not certain that any of the polymorphs had been produced in the pure state, and so some reflections could not be assigned with certainty to any particular phase. Therefore the diffraction pattern was used which was thought to represent the purest state of a particular polymorph and initially only those reflections used which were weaker in the patterns of other fibres containing higher proportions of the other polymorphs. In this way trial unit cells were established for each of the three phases. Between them, these accounted for the observed reflections in all photographs in a way which was consistent with the proportions of the phases thought to be present in any particular fibre.

For the β-phase additional difficulties existed because the highest purity is obtained from gravitationally spun fibre annealed at 150°C, giving a ring pattern unsuitable for unit-cell determination. A fibre drawn to a draw ratio of 5.7 and then annealed at 150°C gives a suitably oriented pattern but containing a mixture of α- and β-phases. *Figure 7a* shows a composite diffraction pattern obtained using both fibres and it is seen that the innermost equatorial reflection does not lie on a ring and so cannot belong to the β-phase. Other reflections not coinciding with rings were similarly rejected. In *Figure 7b* the same oriented fibre is photographed together with as-prepared cast film (the γ-phase). It is seen that the innermost equatorial reflection now coincides with a ring and so this was assigned to the γ-phase.

Because this selective use of reflections was considered somewhat risky, diffraction photographs were taken of biaxially oriented film using a Weissenberg camera, and these were successfully indexed from the proposed cells. Confirmation was also obtained from electron diffractograms from solution-grown single crystals[18,19].

The α-phase unit cell

The α-phase develops as a result of drawing to high orientation. The resulting diffraction patterns are, however, too diffuse for unit-cell determination, and annealing to improve resolution enhances development of the β-phase. The best compromise was achieved using fibre spun with take-up velocity of 400 m min^{-1} annealed under constant length for 2 h at 90°C. The diffraction pattern is shown in *Figure 2*. As already mentioned, only those reflections which certainly belonged to the α-phase were used to fix the trial lattice. This was then used to calculate the expected locations of all other reflections. Those which were observed not to lie near one of these

locations but were in positions, and of such an intensity, that they could reasonably be ascribed to one of the other phases, were rejected from the present considerations. The trial cell parameters were then refined to minimize the discrepancy between the observed and calculated locations of all other reflections. Since the trial lattice was very close to monoclinic, this symmetry was assumed in the refinement.

The unit cell parameters are given in *Table 3* and the observed d-spacings are listed in *Table 4*. The a^*,b^* plane of this cell agrees closely with the electron diffractogram of the platelet solution grown crystal observed by Brisse. The reciprocal parameters of his lattice are $a^* = 0.171$ r.l.u., $b^* = 0.12$ r.l.u., $\gamma^* = 90.0°$ compared with our values of $a^* = 0.170$ r.l.u., $b^* = 0.112$ r.l.u., $\gamma^* = 90.0°$.

It can be seen from *Table 4* that only a few reflections are a poor fit to the calculated lattice. These are ones whose position seems to be sensitive to the presence of other polymorphs, although they cannot be satisfactorily assigned to any other unit cell.

The size of this unit cell is surprising. To match the density of the fibre, six chains must pass through it. With a monoclinic cell, this means that either 3 or 6 of them must be independent, i.e. they cannot be generated from any other chain by a symmetry operation. This seems extremely unlikely. However, almost all reflections fit the calculated positions well, there is good agreement with an electron diffractogram of the ($h\,k\,o$) plane from a single crystal (which also requires 6 chains for correct density) and, as will be shown shortly, the cell is confirmed by the Weissenberg photographs on biaxially oriented sheet. Thus there is strong evidence for the correctness of this cell, and the arrangement of the molecular chains within it must remain unexplained for the time being.

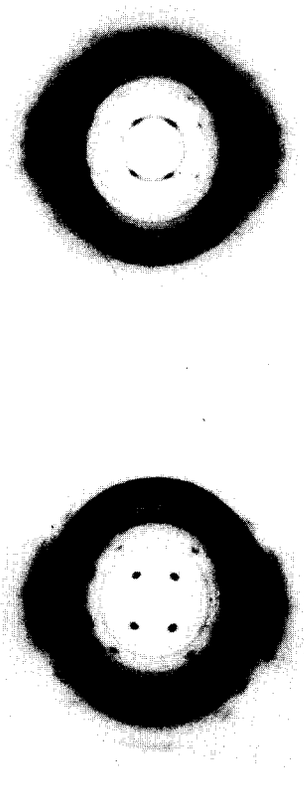

Figure 7 Composite diffraction patterns: (a) gravitationally spun and cold-drawn to draw ratio of 5.7, both annealed at 150°C; (b) fibre cold-drawn to draw ratio of 5.7, then annealed at 150°C with cast film (not annealed)

The β-phase unit cell

Diffraction patterns of two fibres were used for the determination of the unit cell of the β-phase. The first was hot-drawn with a draw ratio of 3, then annealed at 150°C at constant tension for 12 h. This sample had a high proportion of β-phase, the reflections had a fine line width, but it was not particularly well oriented. For this phase the chain axes are tilted slightly away from the fibre axis displacing reflections above and below layer lines. The poor orientation made it difficult to measure this displacement accurately. Consequently the second fibre was used which had a draw ratio of 4, but otherwise received identical treatment. (Its diffraction pattern is shown in *Figure 2*.) In this, there is a higher proportion of α-phase, the reflection line-width is broader, but the high orientation enables accurate measurement to be made of the displacement from the layer lines.

Those reflections which certainly belonged to the β-

Table 3 Unit cell parameters

Phase	Symmetry	Parameters	Volume	No. of chains	Calculated density	Fibre density
α	Monoclinic	a = 9.1Å α = 127.3° b = 17.2Å c = 15.5Å	1930Å^3	6	1.284	1.242
β	Triclinic	a = 4.8Å α = 104.4° b = 5.7Å β = 116.0° c = 15.7Å γ = 107.8°	326Å^3	1	1.262	1.251
γ	Triclinic	a = 5.3Å α = 123.6° b = 13.9Å β = 129.6° c = 15.5Å γ = 88.0°	629Å^3	2	1.308	1.256
Bateman[14]	Triclinic	a = 4.6Å α = 105.5° b = 6.1Å β = 98.5° c = 15.4Å γ = 114.5°	360Å^3	1	1.144	
Joly[15]	Triclinic	a = 10.0Å α = 119.8° b = 9.5Å β = 97.8° c = 15.4Å γ = 95.2°	1240Å^3	4	1.355	1.23 ~ 1.25

Table 4 *d*-Spacings (in Å) of observed reflections, α-phase

l = 0			1			2			3			4			5			6			7		
h	*k*	*d*	*h*	*k*	*d*	*h*	*k*	*d*	*h*	*k*	*d*	*h*	*k*	*d*	*h*	*k*	*d*	*h*	*k*	*d*	*h*	*k*	*d*
1	1	7.56	0	0	12.53	0	0	6.51	0	$\bar{1}$	4.70	1	$\bar{3}$	3.55	1	$\bar{3}$		0	$\bar{7}$		2	$\bar{5}$	
0	2	6.85	1	$\bar{1}$		1	0	5.28	1	$\bar{3}$	4.37	1	$\bar{2}$		0	$\bar{5}$	2.92	2	$\bar{4}$	2.26	1	$\bar{2}$	1.97
1	2	5.50	1	0	7.46	0	1	4.62	1	$\bar{1}$		1	$\bar{1}$	3.27	1	$\bar{4}$		0	$\bar{1}$		2	$\bar{4}$	
0	3	4.52	0	1		2	0	3.71	1	$\bar{4}$	3.90	0	$\bar{5}$		0	$\bar{1}$	2.73	1	$\bar{7}$	2.18	0	$\bar{8}$	
2	0		1	$\bar{2}$	6.07	2	2		2	$\bar{3}$	3.29	2	$\bar{3}$		1	6		1	$\bar{1}$		2	$\bar{6}$	
2	1	4.27	0	$\bar{3}$	5.36	0	$\bar{5}$	3.32	2	$\bar{1}$		1	0	2.91	2	$\bar{3}$	2.56	0	$\bar{8}$	2.07	1	$\bar{8}$	
1	3	4.10	1	$\bar{3}$	4.61	1	2		2	$\bar{4}$	3.12	2	$\bar{2}$		2	$\bar{4}$		0	0		0	$\bar{1}$	1.91
2	2	3.72	2	$\bar{1}$		3	$\bar{1}$		2	0		1	$\bar{6}$	2.69	0	1	2.24	3	$\bar{4}$		2	7	
0	4	3.43	1	2	4.26	3	$\bar{2}$	2.78	0	2	2.83	0	1		2	0		3	5	1.94	0	$\bar{9}$	1.83
2	3	3.20	2	0		1	3		2	1	2.68	2	$\bar{5}$	2.63	3	$\bar{3}$		3	$\bar{3}$		1	0	1.72
1	4		2	1	3.88	0	$\bar{6}$		1	2		3	$\bar{3}$		3	$\bar{4}$		2	$\bar{9}$	1.76	3	$\bar{7}$	
1	5	2.62	2	$\bar{3}$	3.44	3	1	2.56	3	$\bar{3}$		1	$\bar{7}$	2.37	1	1	2.14	1	2				
3	3	2.50	0	$\bar{5}$	3.05	2	$\bar{6}$	2.35	3	$\bar{1}$	2.53	3	$\bar{2}$		0	$\bar{9}$		4	$\bar{6}$	1.67			
0	6		0	4	2.89	1	4		3	4		0	2		2	$\bar{7}$		4	$\bar{2}$				
3	4	2.29	3	1	2.79	4	$\bar{1}$		3	0		4	$\bar{4}$		3	$\bar{2}$							
4	0		3	2	2.6	4	$\bar{2}$	2.16	2	$\bar{6}$		3	$\bar{7}$	1.90	3	$\bar{5}$							
4	1	2.23	2	$\bar{5}$		2	4		0	3	2.40	4	$\bar{1}$		3	$\bar{1}$	2.05						
1	6		3	3	2.34	4	$\bar{3}$		2	2		0	$\bar{9}$		3	$\bar{6}$							
2	6		1	5		3	3	2.09				5	$\bar{1}$		2	1	1.98						
3	5	2.03	3	$\bar{5}$		0	5					3	$\bar{9}$	1.60	0	2							
4	3		4	1	2.16	1	$\bar{8}$	1.92				1	5		4	$\bar{3}$							
1	7	1.91	0	$\bar{7}$		4	2								4	$\bar{4}$	1.82						
4	4		4	$\bar{3}$		4	3	1.79							2	2							
3	6		1	$\bar{7}$	2.09	1	6								4	$\bar{2}$							
5	0	1.81	3	4		5	1								4	$\bar{5}$							
2	7					2	6	1.68							3	1	1.77						
5	1					5	$\bar{4}$								0	3							
															2	$\bar{9}$							
															1	$\bar{10}$	1.69						
															4	0							
															3	$\bar{9}$							
															2	$\bar{10}$	1.60						
															0	4							
															4	1							

Table 5 *d*-Spacings (in Å) of observed reflections. β-phase

l = 0			1			2			3			4			5			6		
h	*k*	*d*	*h*	*k*	*d*	*h*	*k*	*d*	*h*	*k*	*d*	*h*	*k*	*d*	*h*	*k*	*d*	*h*	*k*	*d*
0	1	4.82	0	0	12.30	0	0	6.26	$\bar{1}$	1	3.31	$\bar{1}$	0	3.55	$\bar{1}$	$\bar{1}$	2.74	0	0	
																				2.12
$\bar{1}$	1	4.10	0	$\bar{1}$	5.47	0	$\bar{1}$	5.13	0	$\bar{2}$	2.70	0	$\bar{1}$	3.46	0	0	2.53	$\bar{1}$	1	
1	0	3.72	$\bar{1}$	1	4.15	$\bar{1}$	1	3.78	1	0		0	0	3.13	$\bar{1}$	1	2.39	$\bar{2}$	1	
											2.27									1.97
$\bar{1}$	2	2.62	0	1	3.93	1	$\bar{1}$	3.13	$\bar{2}$	0		$\bar{1}$	$\bar{1}$	2.95	$\bar{2}$	0	2.19	$\bar{1}$	$\bar{2}$	
0	2	2.41	1	$\bar{1}$	3.65	$\bar{1}$	$\bar{1}$	2.95	$\bar{1}$	2	2.18	$\bar{2}$	0		$\bar{2}$	1	2.14			
$\bar{2}$	1	2.12	1	0	3.18	0	$\bar{2}$	2.74	2	$\bar{2}$	1.68	1	$\bar{1}$	2.26	0	3				
																	1.77			
$\bar{2}$	2	2.02	0	$\bar{2}$		1	$\bar{2}$	2.57				0	1		$\bar{1}$	2				
					2.61															
$\bar{1}$	3	1.85	$\bar{1}$	2		$\bar{2}$	1	2.28				$\bar{1}$	2	2.01	1	0				
																	1.68			
$\bar{1}$	$\bar{2}$	1.72	$\bar{2}$	1	2.27	$\bar{2}$	2	2.07				0	$\bar{3}$	1.83	1	$\bar{3}$				
			1	1	2.18	1	1	1.93												
			$\bar{2}$	2	2.10															
			$\bar{1}$	3	1.77															
			$\bar{2}$	3	1.69															

phase were identified and used to construct a trial lattice. Other reflections were then included and the cell parameters were refined as described for the α-phase. The angle by which the chain axes are tilted from the fibre axis, and the axis about which this tilt occurs were estimated from the displacement of the reflections from their layer line positions, and these quantities were included in the refinable parameters.

The unit-cell dimensions are given in *Table 3* and the observed *d*-spacings in *Table 5*. Three reflections could not be indexed with this cell, but they would fit satisfactorily if b^* was halved, doubling the unit cell size and requiring two independent chains per cell. Since there were only three of these reflections, and they were all faint, the two chains can only differ very slightly in conformation, so it was decided to ignore this for the time being. All but a few of the remaining reflections fitted the reciprocal lattice satisfactorily; those which did not were again ones whose position seemed to be sensitive to the proportions of other phases present.

The displacement of reflections caused by tilting is a useful check on the correctness of a unit cell; a mistake will cause the calculated displacement of some reflections to differ in sign or magnitude from that observed. In this case the agreement between observed and calculated displacements was satisfactory for all reflections.

Imperfect crystallization usually causes the measured density to be less than the calculated. In this case they are closer than usual. However, the unit cell densities of the α- and γ-phases are both greater than that of the β, so the presence of these phases would be expected to reduce the difference between the two values.

The γ-phase unit cell

Cast film drawn to a draw ratio of 2.5 and annealed at 80°C for 2 h was used to determine the unit cell of the γ-phase. It was not possible to draw to a higher draw ratio, and annealing at a higher temperature caused conversion to the β-phase. The diffraction pattern is shown in *Figure 3*.

Those spots which correspond with strong reflections of the α- and β-phase, and which did not correspond with a ring in the undrawn, unannealed film were omitted, and a trial net was constructed from the remaining equatorial reflections. This was almost identical with the electron diffractogram of the (*h k o*) plane of the fibrillar solution-grown crystal obtained by Brisse. Since there were only few, diffuse, reflections on the X-ray diffraction pattern it was assumed that the electron diffractogram provided the most accurate values of a^*, b^* and γ^* and these were used with the other layer lines to obtain the remaining parameters. It was necessary to halve b^* to fit all the reflections on these lines. c^*, α^* and β^* were then refined to minimize the discrepancies between the observed and calculated locations of all reflections (except those omitted as described above). These discrepancies were larger than those for the other materials, but this is to be expected because the reflections were more diffuse and difficult to locate accurately.

Confirmation of unit cells using biaxially oriented film

A sheet of material 2 mm thick was compression moulded and quenched in iced water from the press. It was cold-rolled in a series of small reductions until shattering started, when its thickness was almost 0.5 mm, and then annealed for 2 h at 140°C whilst held at constant

Table 6 *d*-Spacings in (Å) of observed reflections. γ-phase

l = 0			1			2			3			4		
h	*k*	*d*	*h*	*k*	*d*	*h*	*k*	*d*	*h*	*k*	*d*	*h*	*k*	*d*
0	2	5.05	0	0	8.52	0	$\bar{1}$	5.59	$\bar{1}$	$\bar{1}$	4.65	$\bar{1}$	$\bar{3}$	3.52
1	$\bar{2}$	3.95	0	$\bar{2}$	7.38	$\bar{1}$	0	5.04	0	$\bar{3}$	3.81	$\bar{1}$	0	3.18
1	0	3.52	0	1	5.54	$\bar{1}$	$\bar{1}$		0	$\bar{4}$	3.27	0	$\bar{3}$	
2	$\bar{2}$		$\bar{1}$	1	4.74	$\bar{1}$	$\bar{2}$	3.76	0	$\bar{5}$	2.80	0	$\bar{4}$	2.58
0	5	2.00	$\bar{1}$	0		0	$\bar{4}$	3.46	$\bar{2}$	$\bar{1}$	2.47	$\bar{1}$	$\bar{4}$	
1	3		0	$\bar{3}$	4.29	$\bar{1}$	2							
1	$\bar{6}$	1.92	$\bar{1}$	$\bar{1}$	3.74									
2	0	1.77	1	4	2.75									
2	$\bar{6}$	1.69	0	3	2.56									
1	4		0	$\bar{5}$	2.35									
			$\bar{2}$	3	2.20									
			2	$\bar{1}$										
			$\bar{1}$	5	2.09									
			2	4										
			$\bar{2}$	0										

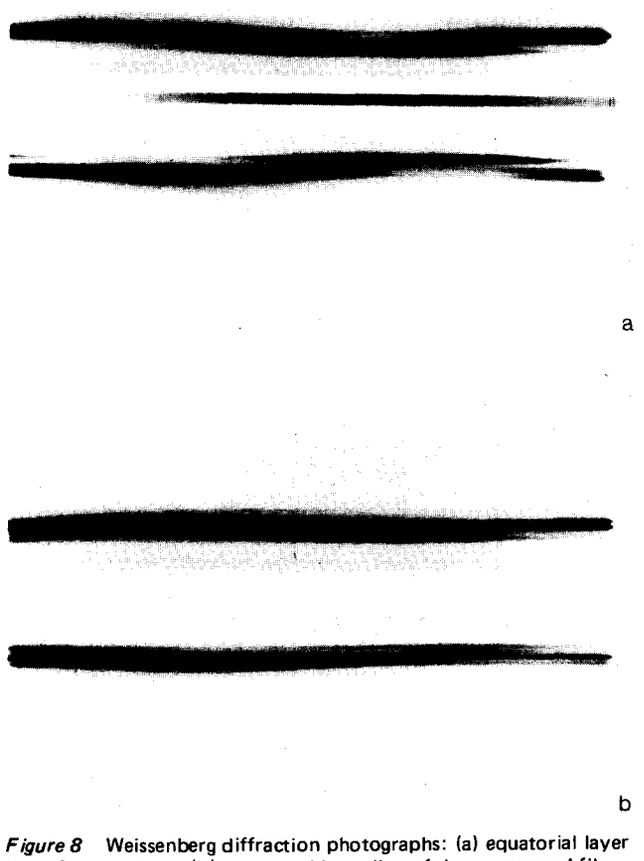

Figure 8 Weissenberg diffraction photographs: (a) equatorial layer line of rolled sheet; (b) equatorial layer line of drawn, pressed film

length. Oscillation and rotation diffraction photographs showed it to have a reasonably high biaxial orientation with the chain axes in the rolling direction, and with a high proportion of the β-phase.

Weissenberg diffraction photographs were taken of the equator, first and second layer lines; that of the equator is shown in *Figure 8a*. From the shortness of the streaks it is clear that the material is reasonably oriented in the plane of the sheet; from the photograph it may also be calculated that b^* is at 70° to the normal to the rolling plane and perpendicular to the direction of rolling.

The reciprocal space coordinates were determined of the points of maximum intensity on the streaks, and these were plotted on a sheet of graph paper. A diagram of the zero-layer reciprocal lattice of the β-phase was overlaid on the graph and it was found that all the strongest reflections lay on this lattice (see *Figure 9*). No reasonable lattice could be drawn to include all the reflections, but those which did not fit the β-phase lattice all lay on that of the α-phase. This procedure was repeated for the first and second layer lines with similar results. In the process of doing this the parameters c^*, α^* and β^* were determined from the Weissenberg photograph and differed from the values corresponding to the cell given in *Table 3* by 0.003 r.l.u., 1.5° and 2.4° respectively. Thus the agreement between the two sets of values is very good.

A further sample was prepared from compression moulded film. The conditions of preparation were exactly the same as for the previous one except that it was initially 0.3 mm thick and was cold-drawn on an 'Instron' tensile testing machine to a draw ration of 4, after which its thickness was 0.14 mm. This specimen had a higher proportion of α-phase than the other, but its orientation in plane of the sheet was not so good. Only the equatorial plane was recorded on Weissenberg photographs and the reflections were very long streaks (*Figure 8b*). The centres of these were used to determine the reciprocal space coordinates which were compared with the zero layer of the α-phase reciprocal lattice as described above. Most fitted the lattice, although accuracy was low because of the poor orientation. Those which did not could be fitted to the β-phase lattice.

Other attempts at unit-cell determination

Two other cell determinations have been reported[14,15], and the parameters are given in *Table 3*. It is seen that they

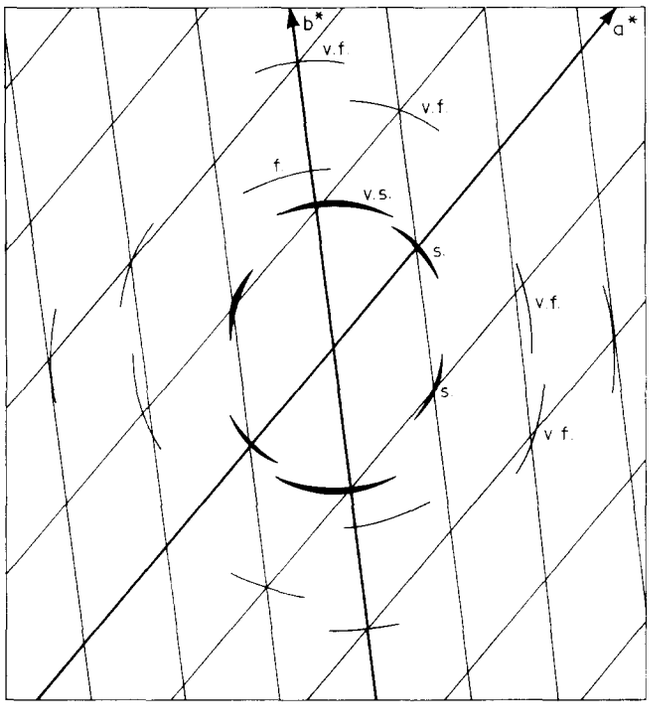

Figure 9 Equatorial Weissenberg diffraction spots from rolled sheet, marked on reciprocal lattice net of β-phase

disagree with the values we have found. Neither appear to have found polymorphism though Bateman *et al.*[14] mention weak reflections which do not fit their lattice. The density of this (1.1445 g cm^{-3}) is lower than that of the bulk material, but that of the lattice of Joly *et al.*[15] (1.355 g cm^{-3}) is greater.

We have tested these proposed unit cells against the diffraction patterns of all the fibres used in our determination and found that neither would fit all the reflections of any of the materials.

Chain packing in the three phases

The cells as given in *Table 3* appear to bear no relationship to each other, but in *Figure 10* their projections on the plane perpendicular to the *c*-axis are superimposed. The lattice points represent points at which molecular chains intersect the plane of the diagram, and it can be seen that this lateral packing differs only slightly between the various allomorphs. It also closely resembles that of 2-GT. The main difference between phases must therefore be the relative axial displacement of neighbouring chains. In the *a*-axis direction, this is 0, 2.1 Å and 3.4 Å for the α-, β- and γ-phases respectively; along the *b*-axis it is 3.5 Å, 1.4 Å and 3.8 Å. The displacements for the β-phase are again nearly equal to those for 2-GT suggesting that these structures are very similar. In the α- and γ-phase cells neighbouring chains will not be regularly displaced and the values given are the average per chain.

SUMMARY AND CONCLUSIONS

There are at least three crystalline phases of 6-GT. In all of them the chain conformation is nearly fully extended and so they must differ mainly in the way in which the chains pack together. The unit cell of each phase has been determined and these are given in *Table 3*. From *Figure 10*, it is clear that the main difference between the phases is the relative axial displacement of neighbouring chains.

It was not found possible to produce any phase in a completely pure state, but conditions were discovered which favoured the development of particular phases. Thus a high stress during crystallization favoured the production of the α-phase in oriented fibres and it appeared to occur with extended chain crystallization. When stress was low the β-phase was favoured and occurred with folded-chain lamellar morphology. If there was a low proportion of α-phase this would recrystallize in the β-phase on annealing, but when there was a high proportion it would be retained whilst new β-phase material crystallized, probably by epitaxial growth on the extended-chain α-phase crystallites. The third, γ-phase, was favoured by precipitation or evaporation from solution.

Electron diffraction experiments on single crystals grown from solution by Brisse[18] confirm the existence of the α- and γ-phases. It is, however, surprising that the α-phase occurs in a platelet crystal grown from solution since our experiments indicate that this phase occurs in fibrillar crystallization under stress.

ACKNOWLEDGEMENTS

We wish to thank Dr R. H. Still of the Department of Polymer and Fibre Science of this University for assistance in synthesizing materials for this study, and also Mr S. R. K. Dauber of the same department for help with spinning and drawing. Thanks are also due to Dr M. Gilbert of the University of Loughborough and to Tennessee Eastman Company, Kingsport, Tennessee for gifts of material. We are grateful to Professor F. Brisse of the University of Montreal for permission to reproduce some of his otherwise unpublished results, and to Dr R.

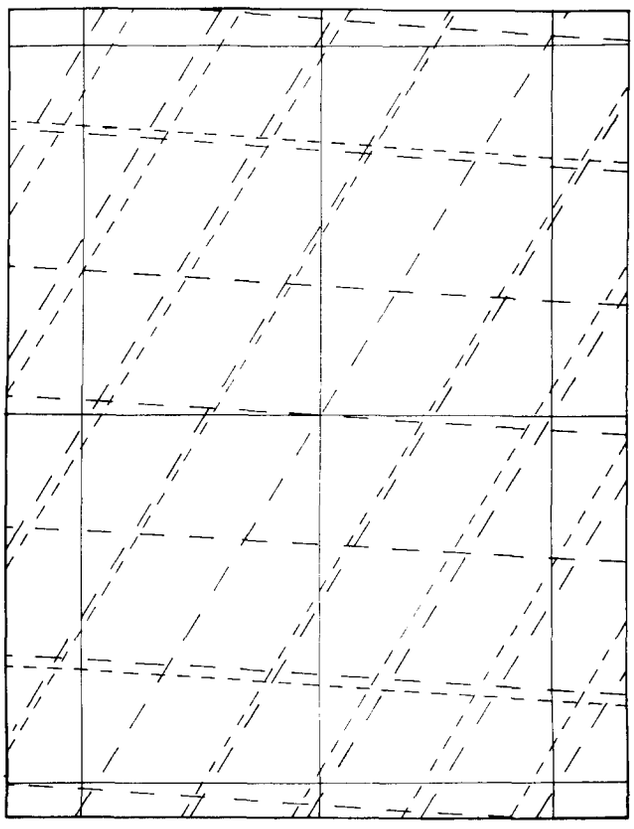

Figure 10 Projections of *a,b* planes of unit cells normal to *c*-axis: α-phase, (———); β-phase, (– – –); γ-phase, (– – – –)

Chandrasekaran of the Department of Biological Sciences, Purdue University, for helpful suggestions during the preparation of the manuscript.

One of us (B.A.I.) gratefully acknowledges a scholarship provided by the Government of the Republic of Iraq.

REFERENCES

1 Hall, I. H. and Pass, M. G. *Polymer* 1976, **17**, 807
2 Yokouchi, M., Sakakibara, Y., Chatani, Y., Tadokoro, H., Tanaka, T. and Yoda, K. *Macromolecules* 1976, **9**, 266
3 Mencik, Z. *J. Polym. Sci., Polym. Phys. Edn.* 1975, **13**, 2173
4 Jakeways, R., Ward, I. M., Wilding, M. A., Hall, I. H., Desborough, I. J. and Pass, M. G. *J. Polym. Sci., Polym. Phys. Edn.* 1975, **13**, 799
5 Boye, C. A. Jr. and Overton, J. R. *Bull. Am. Phys. Soc. Ser. 2* 1974, **19**, 352
6 Brereton, M. G., Davies, G. R., Jakeways, R., Smith, T. and Ward, I. M. *Polymer* 1978, **19**, 17
7 Ward, I. M., Wilding, M. A. and Brody, H. *J. Polym. Sci., Polym. Phys. Edn.* 1976, **14**, 263
8 Hall, I. H., Pass, M. G. and Rammo, N. N. *J. Polym. Sci., Polym. Phys. Edn.* 1978, **16**, 1409
9 Hall, I. H. and Rammo, N. N. *J. Polym. Sci., Polym. Phys. Edn.* 1978, **16**, 2189
10 Desborough, I. J., Hall, I. H. and Neisser, J. Z. *Polymer* 1979, **20**, 545
11 Poulin-Dandurand, S., Perez, S., Revoi, J. F. and Brisse, F. *Polymer* 1979, **20**, 419
12 de P. Daubeny, R., Bunn, C. W. and Brown, C. J. *Proc. Roy. Soc. (A)* 1954, **226**, 531
13 Goodman, I. *Z. Angew. Chem.* 1962, **74**, 606
14 Bateman, J., Richards, R. E., Farrow, G. and Ward, I. M. *Polymer* 1960, **1**, 63
15 Joly, A. M., Nemoz, G., Douillard, A. and Valet, G. *Makromol. Chem.* 1975, **176**, 479
16 Schenk, V. T. *Ph.D. Thesis*, University of Manchester, 1970
17 Hall, I. H. and Ibrahim, B. A. *J. Polym. Sci., Polym. Lett. Edn.* 1980, **18**, 183
18 Brisse, F. and Marchessault, R. H. 'Fiber Diffraction Methods', (Eds. French and Gardner), ACS Symposium Series No. 141 (1980)
19 Poulin-Dandurand, S., Revoi, J-F. and Brisse, F. *Polymer*, to be published